# Bremsstrahlung from an Equilibrating Quark-Gluon Plasma *

Munshi G. Mustafa[1†] and Markus H. Thoma[2‡]
[1] *Institut für Theoretische Physik, Universität Giessen, 35392 Giessen, Germany*
[2] *Theory Division, CERN, CH-1211 Geneva 23, Switzerland*
(January 10, 2014)



## Abstract

The photon production rate from a chemically equilibrating quark-gluon plasma likely to be produced at RHIC (BNL) and LHC (CERN) energies is estimated taking into account bremsstrahlung. The plasma is assumed to be in local thermal equilibrium, but with a phase space distribution that deviates from the Fermi or Bose distribution by space-time dependent factors (fugacities). The photon spectrum is obtained by integrating the photon rate over the space-time history of the plasma, adopting a boost invariant cylindrically symmetric transverse expansion of the system with different nuclear profile functions. Initial conditions obtained from a self-screened parton cascade calculation and, for comparison, from the HIJING model are used. Compared to an equilibrated plasma at the same initial energy density, taken from the self-screened parton cascade, a moderate suppression of the photon yield by a factor of one to five depending on the collision energy and the photon momentum is observed. The individual contributions to the photon production, however, are completely different in the both scenarios.

PACS numbers: 12.38.Mh, 24.10.Nz, 25.75.-q

Typeset using REVTEX

*Supported by BMBF, GSI Darmstadt, DFG, and Humboldt foundation

†Humboldt fellow and on leave of absence from Saha Institute of Nuclear Physics, 1/AF Bidhan Nagar, Calcutta 700 064, India

‡Heisenberg fellow

## I. INTRODUCTION

In ultrarelativistic heavy ion collisions photons are emitted during the entire life time of the fireball. Since their mean free path is large compared to the size of the fireball [1], energetic photons escape from it without any interaction. Therefore photons with large transverse momenta probe the early, hot stage of the collision and may serve as a direct signature for the quark-gluon plasma (QGP) formation at RHIC and LHC [2]. In order to use photons as a probe for the QGP, we have to predict the thermal spectrum from the QGP as well as from the hadronic phase. For this purpose we have to convolute the photon production rates from both phases with the space-time evolution of the fireball. Here we want to focus on a QGP phase possibly created at RHIC and LHC energies. Recent calculations of the photon production rate from the QGP, taking into account bremsstrahlung, resulted in a significantly larger rate compared to previous investigations [3]. These rates have been implemented in a hydrodynamical calculation assuming a local thermal and chemical equilibrium [4,5]. However, at RHIC and LHC the QGP phase is not expected to be in chemical equilibrium, *i.e.*, the phase space of quarks and gluons will be undersaturated probably [6–8]. Using non-equilibrium photon rates without bremsstrahlung and generalizing the hydrodynamical calculations to chemical non-equilibrium, the photon spectrum from a chemically non-equilibrated QGP has been estimated [9–11]. Due to the undersaturation in particular of the quark component a suppression of the photon yield has been observed [10]. In order to make up-to-date predictions for the thermal photon spectrum of a QGP at RHIC and LHC, the both competing effects of the enhanced photon rate considering bremsstrahlung and the reduction of the photon yield due to the chemical non-equilibrium should be combined. This is the aim of the present investigation.

In the next section we present an estimate of the non-equilibrium photon rates taking into account bremsstrahlung. In Sec.III we summarize briefly our hydrodynamical description, before we will discuss our results in Sec.IV and draw our conclusions in Sec.V.

## II. PHOTON PRODUCTION FROM QUARK-GLUON PLASMA

The production rate of energetic real photons in an equilibrated QGP has been calculated using the Hard Thermal Loop (HTL) resummation technique [12,13]. Here only the lowest order contributions, namely quark-antiquark annihilation and Compton scattering (corresponding to a one-loop polarization tensor containing a HTL resummed quark propagator in the case of a soft quark momentum), has been taken into account. An estimate for these contributions in chemical non-equilibrium has been given by computing these rates from the tree level scattering diagrams and using off-equilibrium distribution functions for the external quarks and gluons [10]. For this purpose the equilibrium distributions have been multiplied by space-time dependent fugacity factors $\lambda_{g,q}$ describing the deviation from equilibrium according to Ref. [6,14]. Also the infrared cutoff in these rates given by the effective in-medium quark mass has been generalized to non-equilibrium. Neglecting Pauli blocking and Bose enhancement effects, which is justified since the average momenta of the partons is $3T$ in the baryon free QGP, the following result for the rates due to Compton scattering and quark-antiquark annihilation has been obtained [9,11],

$$E\frac{\mathrm{d}N_\gamma}{\mathrm{d}^4x\,\mathrm{d}^3p}\bigg|^{\mathsf{ceq.}}_{\mathsf{com.}} = \frac{2\alpha\alpha_s}{\pi^4}\lambda_q\lambda_g T^2\left(\sum_f e_f^2\right)e^{-E/T}\left[\ln\left(\frac{4ET}{\kappa_c^2}\right)+\frac{1}{2}-C\right], \tag{1}$$

and

$$E\,\frac{\mathrm{d}N_\gamma}{\mathrm{d}^4x\,\mathrm{d}^3p}\bigg|^{\mathsf{ceq.}}_{\mathsf{ann.}} = \frac{2\alpha\alpha_s}{\pi^4}\lambda_q\lambda_{\bar{q}} T^2\left(\sum_f e_f^2\right)e^{-E/T}\left[\ln\left(\frac{4ET}{\kappa_c^2}\right)-1-C\right]. \tag{2}$$

Here $C = 0.577216\ldots$, and $\kappa_c = 2m_q^2$, where the thermal mass of the quarks in the non-equilibrated medium is given as

$$m_q^2 = \frac{4\pi\alpha_s}{9}\left(\lambda_g+\frac{\lambda_q}{2}\right)T^2. \tag{3}$$

Alternatively non-equilibrium rates can be calculated by generalizing the HTL technique to quasistatic chemical non-equilibrium situations [15,16]. In the case of the photon production rate this more consistent, but also more elaborate, method leads to quantitatively very similar results as the simplification used above [15].

Recently Aurenche et al. [3] have shown that there are additional contributions to the thermal photon rate at the same order $\alpha_s$ coming from two-loop diagrams within the HTL method. The corresponding physical processes are bremsstrahlung and quark-antiquark annihilation, where the quark (or antiquark) scatters of a parton from the QGP. The latter process becomes important especially for energetic photons as the rate is proportional to $ET$, whereas the rates from bremsstrahlung, annihilation without rescattering, and Compton scattering are proportional to $T^2$. Although the Compton and annihilation contributions are enhanced in the weak coupling limit by a logarithmic factor $\ln(1/\alpha_s)$ compared to the bremsstrahlung processes, the latter ones dominate for realistic values of the coupling constant by a factor of 5 or more [3,4]. Of course, the extrapolation of these perturbatively calculated rates to realistic values of the coupling constant, for which we will use $\alpha_s = 0.3$ in the following, is questionable. However, in view of the lack of other methods for calculating dynamical quantities such as production rates in thermal field theory so far, we assume that these results can be used as a rough estimate at least in the case of high energy photons ($E \gg T$), in which we are interested.

For estimating the bremsstrahlung contributions to the non-equilibrium rate we adopt the same approximations as in (1) and (2). This means that we start from the scattering diagrams corresponding to these processes and ascribe non-equilibrium distributions to the external partons in the entrance channels. Restricting ourselves to $t$-channel diagrams, which dominate because the exchanged gluon is soft [3], and considering the different spin, color, and flavor ($N_f = 2$) factors, we find for the bremsstrahlung process

$$E\,\frac{\mathrm{d}N_\gamma}{\mathrm{d}^4x\,\mathrm{d}^3p}\bigg|^{\mathsf{ceq.}}_{\mathsf{brem.}} = \frac{2N_cC_F}{\pi^5}\alpha\alpha_s\left(\frac{4}{7}\lambda_q^2+\frac{3}{7}\lambda_g\lambda_q\right)\left(\sum_f e_f^2\right)T^2e^{-E/T}(J_T-J_L)\ln(2)\ , \tag{4}$$

and for the annihilation with scattering process

$$E\,\frac{\mathrm{d}N_\gamma}{\mathrm{d}^4x\,\mathrm{d}^3p}\bigg|^{\mathsf{ceq.}}_{\mathsf{aws}} = \frac{2N_cC_F}{3\pi^5}\alpha\alpha_s\left(\frac{2}{5}\lambda_q^3+\frac{3}{5}\lambda_g\lambda_q^2\right)\left(\sum_f e_f^2\right)ETe^{-E/T}(J_T-J_L)\ . \tag{5}$$

Here the constants $J_T \simeq 4.45$ and $J_L \simeq -4.26$ for two flavors are the same as in equilibrium, since their dependence on the fugacities can be neglected. For they are functions of $m_q/m_g$ only and the square of the effective quark mass $m_q^2$, Eq.(3), and of the effective gluon mass $m_g^2$ are proportional to the gluon fugacity, if the much smaller quark fugacity is neglected. It should be noted that in Eq.(5) the combination of the different parton fugacities appears in cubic power, instead of quadratically as for the other processes, due to the fact that this particular process involves three particles in the entrance channel.

## III. HYDRODYNAMIC EXPANSION AND CHEMICAL EQUILIBRATION

To evaluate the thermal photon spectrum one has to convolute these emission rates with the space time history of the expanding fireball out of chemical equilibrium. We do not want to repeat here the calculations of the chemical evolution of the QGP by means of rate equations [6] and its implementation in a hydrodynamical code, but refer the reader to Ref. [11,14]. In this hydrodynamical model, which we are adopting here, the transverse expansion of the QGP has been taken into account.

The essential input needed are the initial conditions for the fugacities and temperature at the time at which local thermal equilibrium is achieved. In order to take into account the uncertainties in these initial conditions we consider various possibilities predicted by two microscopic models for ultrarelativistic heavy ion collisions, namely SSPC [17] and HIJING [8]. The initial conditions we are using here are tabulated in Tab.I. The ones denoted by (I) are the original HIJING predictions, while the set (II) is obtained by multiplying the original initial fugacities by a factor of 4 and by decreasing the initial temperature somewhat, in order to take into account possible uncertainties in the model such as the neglect of soft parton production from the color field [11].

In addition to the different initial conditions, we also need a nuclear profile function for the fireball to solve the hydrodynamical equations numerically as matter distributions with sharp edges are difficult to use in numerical simulations [18]. Another aim of our investigation is to study the dependence of the photon spectra on different choices of the profile function. For this purpose we consider in the following two profile functions. The first one is a Fermi-like profile function [18]

$$T_A(r) = \frac{1}{e^{(r-R_T)/\delta}+1} \quad , \tag{6}$$

where $r$ is the transverse coordinate, $R_T$ is the transverse radius of the nucleus and $\delta$ is the surface thickness, which has also been used in Ref. [11]. The second one is the wounded-nucleon profile [19] given by

$$T_A(r) = \frac{3}{2}\sqrt{1-\frac{r^2}{R_T^2}} \quad . \tag{7}$$

Since the initial conditions shown in Tab.I describe averages over the transverse cross section, $\pi R_T^2$, of the colliding nuclei in a central collision, one needs to modify them for different nuclear profiles. This implies that the system will have higher initial energy density and fugacities using the wounded-nucleon profiles, but also the preexistence of a density gradient over the whole transverse area resulting in a faster onset of the transverse expansion throughout the plasma volume [19].

## IV. RESULTS

In Fig.1 we present the thermal photon production from the quark phase as a function of its transverse momentum at RHIC energies with SSPC initial conditions and the Fermi-like profile function both in the equilibrium and equilibrating scenario, where we assumed the same initial energy densities in both cases given in Tab.I. The initial temperature in the equilibrium case corresponding to $\epsilon_i = 61.4$ GeV/fm$^3$ is $T_i^{eq} = 0.429$ GeV. Therefore there is an interplay in the photon production between the enhanced temperature and the reduced fugacities in the non-equilibrium. As a result the total photon yield is suppressed at $p_T = 1$ GeV by a factor of five but almost identical at $p_T = 5$ GeV in the equilibrating compared to the equilibrated scenario. Keeping, however, the initial temperature ($T_i = 0.668$ GeV) instead of the initial energy density fixed leads to a strong reduction of the non-equilibrium compared to the equilibrium rate by one (low $p_T$) to three (high $p_T$) orders of magnitude. The strong suppression at high $p_T$ is due to the small fugacities in the early hot stage, from which the energetic photons are emitted mainly. Keeping, however, the initial energy density fixed this effect is counterbalanced by the higher initial temperature in the non-equilibrated case.

The contribution from different physical processes discussed in the preceding section can easily be identified from Fig.1 itself. As expected from the equilibrium static rates, the photon spectrum from the equilibrated QGP (see upper panel of Fig.1) is dominated by the annihilation with scattering contribution. In the case of a chemically equilibrating plasma (lower panel of Fig.1) the most dominant contribution comes from the usual bremsstrahlung processes, even though the *aws* static equilibrium rate was higher by almost an order of magnitude. The reason is obvious as the rate for the *aws* processes for an equilibrating plasma involves the parton fugacities to cubic power (Eq.(5)) whereas the other processes are only quadratic in the fugacities (Eqs.(1,2,4)), and the fugacities at RHIC are small for the entire life time of the plasma. At higher $p_T$ the Compton and annihilation one-loop contributions even exceed clearly the *aws* contribution as energetic photons have their origin in the early hot stage of the plasma, where the fugacities are very small. It is also worthwhile to note that the SSPC model predicts a gluon dominated plasma implying larger contributions from processes involving gluons in the entrance channel.

The total thermal photon yield at RHIC dominates over the prompt photon contributions [20] for $p_T \leq 4.5$ GeV. However, if only the Compton and annihilation contributions are considered [11] the prompt photons overshadow the thermal photon yield already beyond $p_T \geq 3$ GeV. Since the life time of the plasma at RHIC is small, the photon yield is not affected by flow [11].

The corresponding results for LHC energies are shown in Fig.2. Here the non-equilibrium rate is suppressed compared to the equilibrium at the same initial energy density ($T_i^{eq} = 0.695$ GeV) by about a factor of three for all photon momenta and by one to two orders of magnitude in the case of the same initial temperature. The photon yields from different processes as well as the total yield are much larger than at RHIC as the life time of the plasma, likely to be created at LHC energy, is expected to be much larger and the initial temperature and fugacities are higher. The upper panel shows the equilibrated scenario, whereas the lower panel applies to the equilibrating one. Now the usual bremsstrahlung and the *aws* contribution originating from two-loop calculations are similar in the non-equilibrium

case, whereas the one-loop contribution is smaller at all $p_T$. The reduced suppression of the *aws* contribution compared to RHIC can be understood in the following way. The rate depends linearly on the temperature and cubicly on the fugacities. In addition the *aws* is also proportional to the energy of the photon. Now with the passage of time the system expands, the temperature falls and the chemical reactions pushes the system towards equilibrium causing the fugacities to increase, though at later time they decrease significantly caused by transverse expansion. Hence, there is a competition between the space-time evolution of the temperature and the fugacities though they are not exactly counterbalanced. Rather, the interplay of these two quantities along with the photon energy dependence causes a reduced suppression of the *aws* contribution compared to RHIC.

The prompt photon productions [20] due to lowest order QCD (Born) and inclusive photons (background photons fragmented off high-$p_T$ quark jets) will remain buried under the thermal photon yield for all $p_T$-values considered here.

Comparing the photon spectra obtained with the wounded-nucleon profile we observe that the photon yield following from the Fermi-like profile is a little bit higher. This enhancement, which is always less than a factor of two, is caused by the fact that a Fermi-like profile associated with a slower cooling implies a higher temperature.

In the following we present our results with HIJING initial conditions. If we use the original prediction, *i.e.*, HIJING-I, then the life time of the QGP phase is very small (less than 2 fm/c) for RHIC and 7.5 fm/c for LHC [11]. Also the matter will be very dilute due to the very small initial values of the fugacities at RHIC. Furthermore, for LHC only the fluid beyond 4 fm from the centre participates in flow. Now for HIJING-II initial condition, the life time of the plasma increases substantially both for RHIC ($\sim$ 4 fm/c) and LHC ($\sim$ 12 fm/c). Also the initial fugacities differ by one order of magnitude for RHIC, and are reasonably higher for LHC. For LHC the entire fluid will participate in the transverse flow since the life time is large and initially the system will approach equilibrium but then be driven away from it as soon as the large transverse velocity gradient develops. Fig.3 exhibits the photon production from the equilibrating plasma with HIJING-I initial conditions and a Fermi-like nuclear profile both at RHIC (upper panel) and LHC (lower panel) energies. Because of the low values of the fugacities during the entire life time of the plasma [11], the contribution of the different processes as well as the total yield are strongly suppressed compared to the case using SSPC initial conditions. In particular there is a huge suppression of the *aws* contribution, depending cubicly on the fugacities, compared to the other processes at RHIC. Also at LHC the strong suppression of the *aws* contribution at high-$p_T$ is due to the very small initial fugacities as high-$p_T$ photons are mostly emitted from the initial stages.

Finally the results for an equilibrating plasma with HIJING-II initial conditions are given in Fig.4. Since the initial fugacities are an order of magnitude higher for RHIC (upper panel), the contributions from each process, particularly from the *aws*, are enhanced substantially compared to HIJING-I. Since the initial fugacities are higher compared to SSPC but the initial temperature is smaller, there is a counterbalance of these two effects, and the total photon production for LHC (lower panel) is almost the same as that using SSPC initial conditions (lower panel of Fig.2).

## V. SUMMARY AND CONCLUSION

We have considered the photon production from a chemically non-equilibrated QGP at RHIC and LHC energies. As a new aspect we have included bremsstrahlung processes. The photon production rate due to these processes has been calculated recently using the HTL resummation technique by Aurenche et al. [3] in the case of a fully equilibrated QGP. Instead of repeating this calculation in the non-equilibrium plasma, we estimated the non-equilibrium photon production rate in the following way: we simply assigned fugacity factors, describing the deviation of the parton densities from chemical equilibrium, to the partons in the entrance channels of the matrix elements corresponding to the different processes (annihilation, Compton scattering, bremsstrahlung, annihilation with scattering). In the case of the first two processes this approach has to be shown to give quantitatively very similar results as the more elaborate HTL method extended to chemical non-equilibrium [15]. Moreover, regarding the uncertainties, such as the validity of perturbation theory and the initial conditions in the computation of the photon spectrum, this simplification is justified.

The photon spectra have been calculated from these rates by using a hydrodynamical calculation, describing the space-time evolution of the QGP phase of the fireball, where we have taken into account the transverse expansion of the fireball. The initial conditions for the temperature and the fugacities have been taken from microscopic models (SSPC, HIJING).

We found that the photon yield is reduced by a factor one to five depending on the collision energy and photon momentum compared to the fully equilibrated plasma, assuming the same initial energy density taken from the SSPC model. This moderate suppression is the result of the interplay between the small fugacities and the increased temperature in the non-equilibrium compared to the equilibrium scenario. In general the suppression is more pronounced for energetic photons coming from the highly dilute early stage.

Assuming the same initial temperature the photon yield from the non-equilibrium QGP is reduced by one to three orders of magnitude. The reason for this large difference is the reduction of the initial temperature for the equilibrated scenario assuming a fixed initial energy density. In ultrarelativistic heavy ion collisions assuming free flow the initial energy density is determined from the measured particle multiplicity, which is related to the collision energy [21]. Therefore the assumption of a fixed initial energy density instead of temperature appears to be more physical.

Although the total photon yield does not differ much in the both scenarios, using the same initial energy density, its composition by the individual processes is completely different. Whereas the contribution from the annihilation with scattering process dominates the photon production over the entire momentum range in equilibrium, in a chemically non-equilibrated plasma it is suppressed at RHIC energies compared to the bremsstrahlung contribution, which is now dominating, and even to the one-loop (annihilation, Compton scattering) contributions, which is the smallest in equilibrium. The reason for this behavior is that the annihilation with scattering process depends cubicly on the fugacities, which are very small at RHIC, whereas the other processes only quadratically. At LHC energies, on the other hand, where the fugacities are significantly larger, the annihilation with scattering and the bremsstrahlung contributions are of the same order and exceed the one-loop

contributions clearly.

We have also investigated the dependence of our results on different initial conditions and the choice of the profile of the fireball. The photon yield can vary by more than an order of magnitude, depending on the choice of the initial conditions, while the dependence on the profile function is weak.

Although in this investigation all important effects (bremsstrahlung, chemical non-equilibrium, transverse expansion), known so far, are incorporated, there are still uncertainties and open questions. For example, the applicability of perturbative methods and the role of higher order contributions is unknown. Also a consistent treatment of the chemical equilibration, the space-time evolution of the fireball, and the non-equilibrium photon rates within the framework of the kinetic theory would be desirable.

## ACKNOWLEDGMENTS

The authors are grateful to H. Zaraket for helpful discussions concerning the extension of the bremsstrahlung rate to non-equilibrium.

# REFERENCES


[1] M. H. Thoma, Phys. Rev. D **51**, 862 (1995).
[2] see for example, P.V. Ruuskanen, Nucl. Phys. A **544** (1992) 169c.
[3] P. Aurenche, F. Gelis, R. Kobes, and H. Zaraket, Phys. Rev. D **58**, 085003 (1998).
[4] D. K. Srivastava, Eur. Phys. J. C **10**, 487 (1999). D.K Srivastava and B. Sinha, Eur. J. Phys. C **12**, 109 (2000).
[5] F. D. Steffen, ⟨nucl-th/9909035⟩.
[6] T. S. Biró, E. van Doorn, B. Müller, M. H. Thoma, and X.-N. Wang, Phys. Rev. C **48**, 1275 (1993).
[7] L. Xiong and E. Shuryak, Phys. Rev. C **49**, 2203 (1994).
[8] X.-N. Wang, Phys. Rep. **280**, 287 (1997).
[9] M. Strickland, Phys. Lett. B **331**, 245 (1994).
[10] C. T. Traxler and M. H. Thoma, Phy. Rev. C **53**, 1348 (1996).
[11] D. K. Srivastava, M. G. Mustafa, and B. Müller, Phys. Rev. C **56**, 1064 (1997).
[12] J. I. Kapusta, P. Lichard, and D. Seibert, Phys. Rev. D **44**, 2774 (1991).
[13] R. Baier, H. Nakkagawa, A. Niegawa, and K. Redlich, Z. Phys. C **53**, 433 (1992).
[14] D. K. Srivastava, M. G. Mustafa, and B. Müller, Phys. Lett. B **396**, 45 (1997).
[15] R. Baier, M. Dirks, K. Redlich and D. Schiff, Phys. Rev. D **56**, 2548 (1997).
[16] M. E. Carrington, H. Defu, and M. H. Thoma, Eur. Phys. J. C **7** (1999) 347.
[17] K. J. Eskola, B. Müller, and X.-N. Wang, Phys. Lett. B **374**, 20 (1996).
[18] H. von Gersdorff, L. McLerran, M. Kataja, and P. V. Ruuskanen, Phys. Rev. D **34**, 794 (1986).
[19] B. Müller, M. G. Mustafa and D. K. Srivastava, Heavy Ion Physics **5**, 387 (1997).
[20] J. Cleymans, E. Quack, K. Redlich, and D. K. Srivastava, Int. J. Mod. Phys. A **10**, 2941 (1995).
[21] H. Satz, Nucl. Phys. A **544**, 371c (1992).

## TABLES

TABLE I. Initial conditions for the hydrodynamical expansion phase in central collision of two gold nuclei at BNL RHIC and CERN LHC energies from SSPC and HIJING models.

| Energy | $\tau_i$ ($\mathrm{fm}/c$) | $T_i$ (GeV) | $\lambda_g^{(i)}$ - | $\lambda_q^{(i)}$ - | $\epsilon_i$ ($\mathrm{GeV/fm^3}$) |
|---|---|---|---|---|---|
| **SSPC** | | | | | |
| RHIC | 0.25 | 0.668 | 0.34 | 0.064 | 61.4 |
| LHC | 0.25 | 1.02 | 0.43 | 0.082 | 425 |
| **HIJING** | | | | | |
| RHIC, I | 0.7 | 0.55 | 0.05 | 0.008 | 4.0 |
| RHIC, II | 0.7 | 0.40 | 0.53 | 0.083 | 11.7 |
| LHC, I | 0.5 | 0.82 | 0.124 | 0.02 | 48.6 |
| LHC, II | 0.5 | 0.72 | 0.761 | 0.118 | 176 |

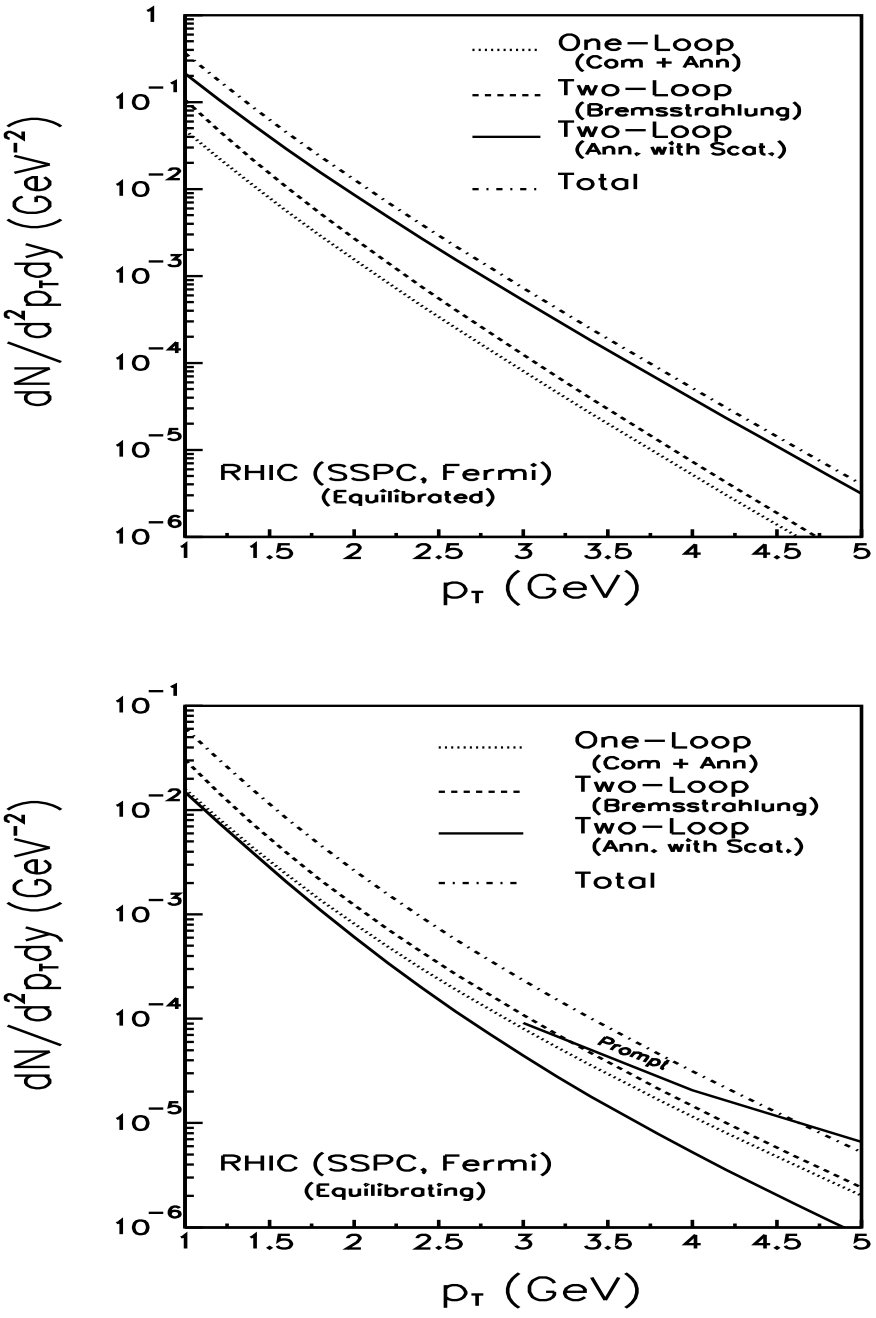


FIG. 1. Photon spectra from various processes at RHIC energies with SSPC initial conditions and the Fermi-like profile function. The upper panel represents the fully equilibrated scenario, whereas the lower panel corresponds to the chemically equilibrating scenario.

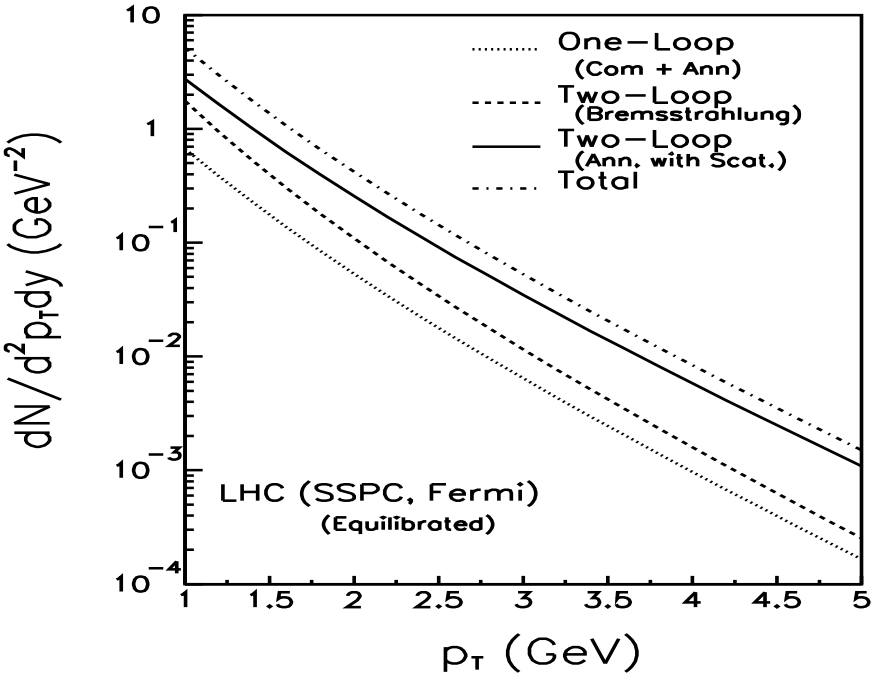


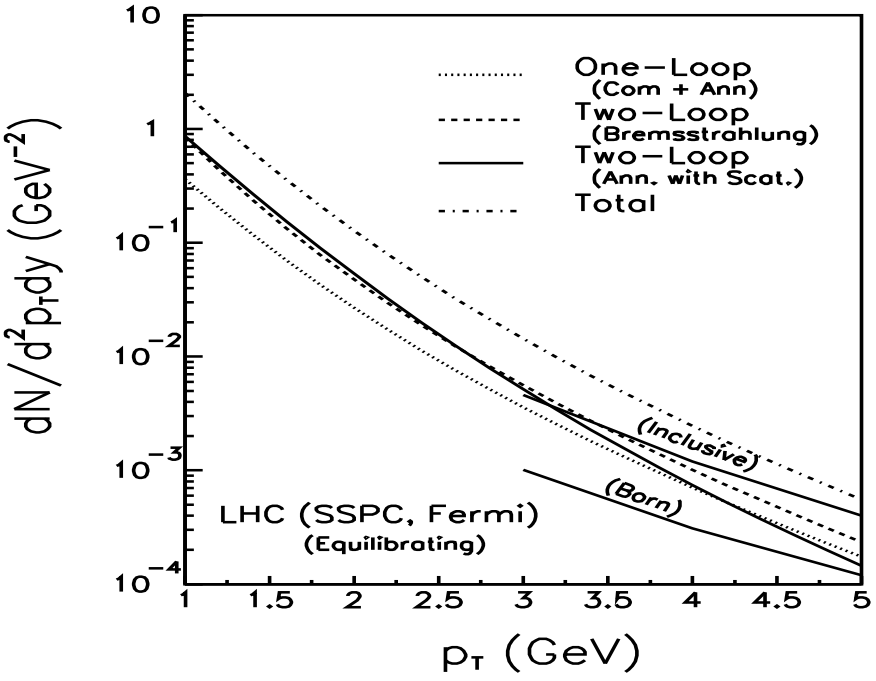


FIG. 2. Same as Fig.1 for LHC energies.

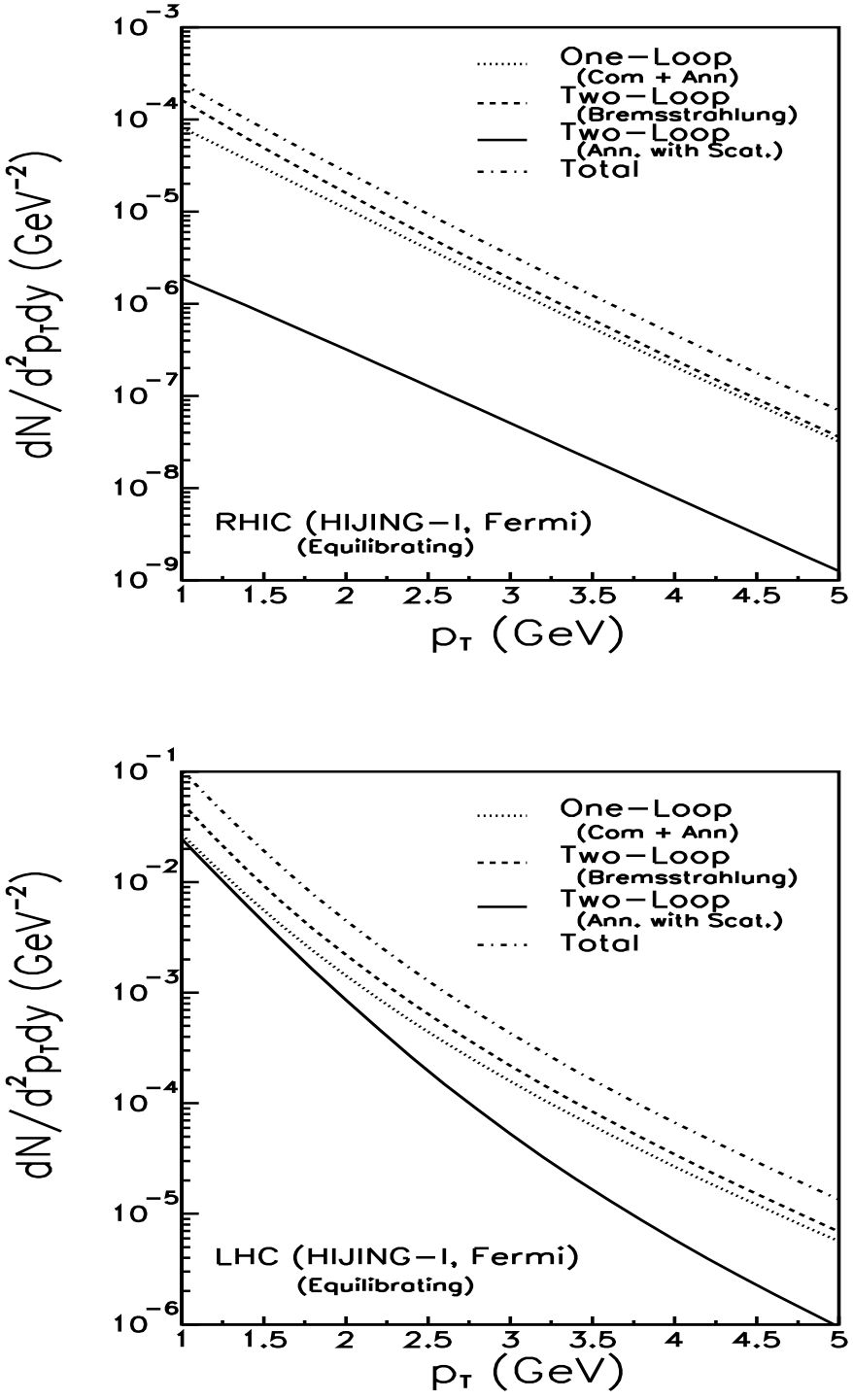


FIG. 3. Photon spectra for a chemically equilibrating plasma at RHIC (upper panel) and LHC (lower panel) energies with HIJING-I initial conditions and the Fermi-like profile function.

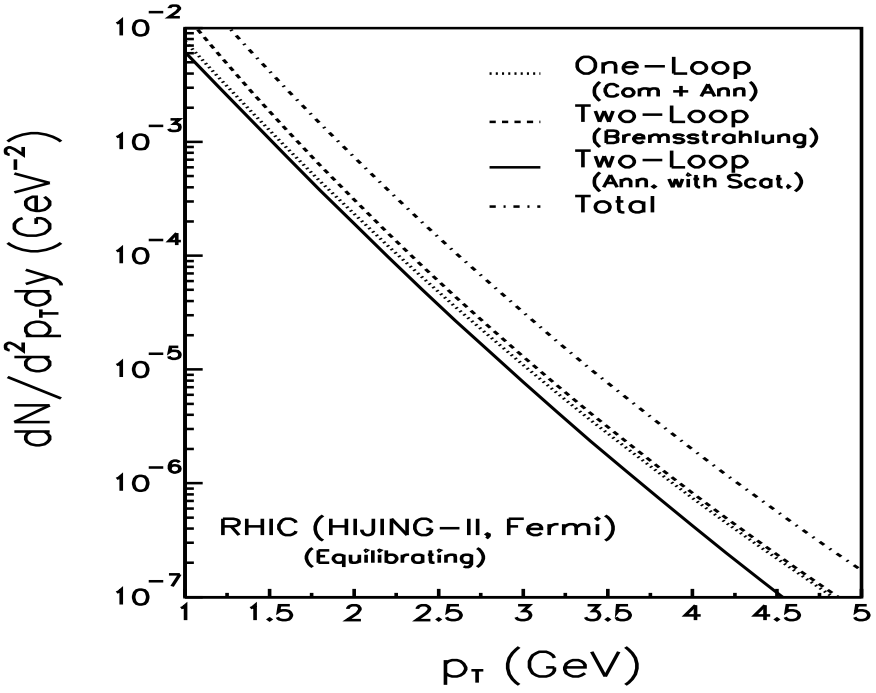


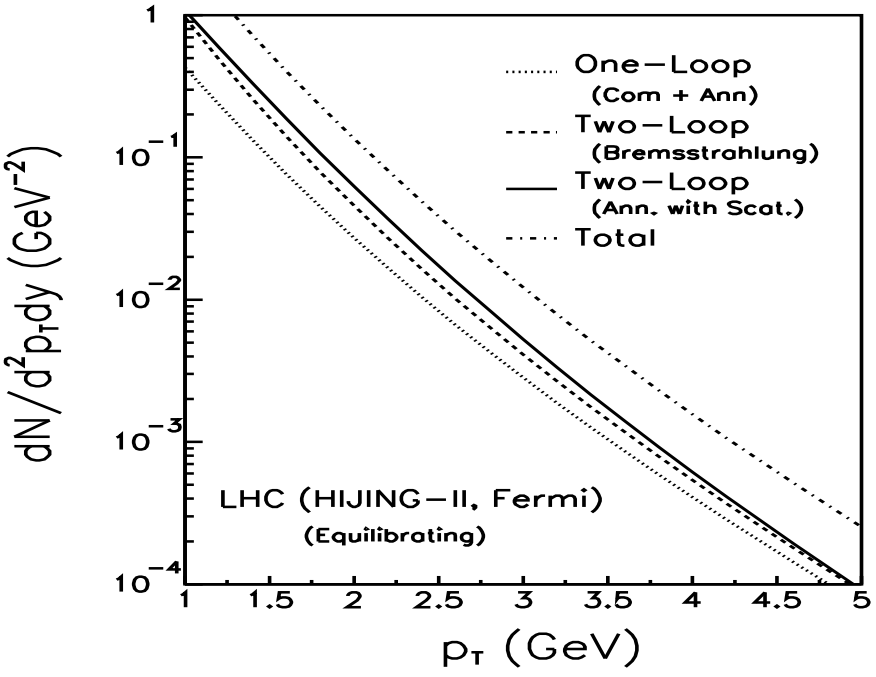


FIG. 4. Same as Fig.3 with HIJING-II initial conditions.